Evaluation of Robotic Needle Insertion in Conjunction with *in Vivo* Manual Insertion in the Operating Room

T.K. Podder[1], J. Sherman[1], D.P. Clark[1,4], E.M. Messing[2], D.J. Rubens[3], J.G. Strang[3], L. Liao[3], R.A. Brasacchio[1], Y. Zhang[1], W.S. Ng[5], and Y. Yu[1,4]

Departments of [1]Radiation Oncology, [2]Urology, and [3]Radiology,
University of Rochester Medical Center, Rochester, NY 14642, USA.

[4]Department of Biomedical Engineering
University of Rochester, Rochester, NY 14642, USA.

[5]Department of Mechanical and Aerospace Engineering,
Nanyang Technological University, Singapore 639798.
tarun_podder@urmc.rochester.edu

Abstract: *Precise interstitial intervention is quite challenging because of several reasons. Researchers have reported in vitro needle insertion forces encountered while steering through soft tissue and soft material phantoms. Hardly any in vivo force measurement data is available in the literature. In this paper, we present needle insertion forces and torques measured during actual brachytherapy procedure in the operating room (OR). We highlight human factors involved in the surgical needle intervention during prostate seed implant (PSI) procedures. We believe that some of the issues can be eliminated or reduced using a robotic system. We have also presented in vitro data during robotic needle insertion into animal soft tissue phantoms and compared with manual insertions.*

I. INTRODUCTION

Many medical diagnostic and therapeutic procedures like tissue biopsy, brachytherapy, anaesthesia, vaccinations, blood/fluid sampling, abscess drainage, catheter insertion, cryogenic ablation, electrolytic ablation, neurosurgery, deep brain biopsy etc. require percutaneous intervention of surgical needles. Accurate placement of needle for these procedures is very important. But accurate steering and placement of different types of surgical needles in soft tissues are challenging because of several reasons such as tissue heterogeneity, anisotropy, nonlinear viscoelasticity, relaxation, tissue deformation and deflection, unfavorable anatomic structures, needle bending, inadequate sensing, and poor maneuverability. Therefore, understanding of the complex mechanism of needle interaction with living biological tissues is an area of active research.

In 2005, the American Cancer Society (ACS) has estimated 232,090 new patients will be diagnosed with prostate cancer; it is about 33% of all cancers among men in the United States [1]. Brachytherapy is one of the most commonly practiced and popular modalties of prostate cancer treatment. In this procedure, radioactive seeds are deposited and remain permanently in the prostate gland to kill and restrict the cancerous cells. The radiation exposure to the target and other vital organs (urethra, rectum, bladder, etc.) depends on the placement accuracy of the needles (17-gauge/18-gauge, i.e. 1.473mm/1.27mm in diameter and 200mm in length), which deliver the seeds. These needles are inserted through the perineum and pass through different tissues before entering into the prostate gland (Figure 1).

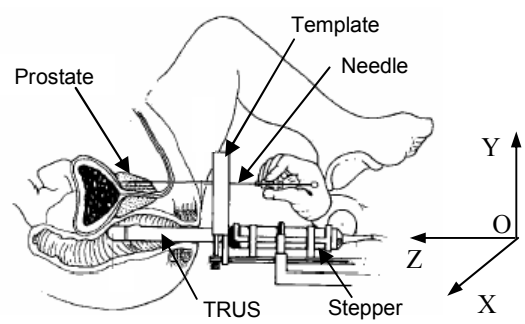

Figure 1: Prostate Brachytherapy (Seattle method).

In brachytherapy, positional accuracy of the radioactive seeds is very important for optimizing the dose delivery to the targeted cancerous tissues sparing the critical organs and structures. In currently practiced procedures, the fixed grid holes spaced 5mm apart in the template allow the surgeon to insert the needle at specified fixed positions. Very little can be done to steer the needle to a place other than straight passing through the hole in the template. Change in needle insertion position may be required

based on intraoperative dynamic planning. Sometimes, especially for larger prostates, the needle needs to be angulated to avoid pubic arch interference (PAI) and get access to the desired target position in the prostate for seed delivery. In current brachytherapy procedure with fixed template the needle angulation is almost impossible. However, the surgeon can use a hook to bend the needle and get to the desired position after several trials. Whereas a robotic system, which does not require the template, can provide flexibility in positioning and orientating (angulating) along with improved accuracy of needle insertion and seed deposition. Robotic system can assist surgeons and reduce fatigue. Additionally, with the assistance of robotic system, less skillful surgeons will be able to treat patients with higher quality.

Recently, several researchers are developing robotic systems for permanent seed implant (PSI) in the prostate [2]-[4]. To design and control any robotic system, the design and control engineers must know the robotic workspace, motion profile, and force-torque that will be encountered by the system. Especially for prostate brachytherapy procedures the workspace analysis and the assessment of force-torque encountered by the needle insertion mechanism are critical mainly because of two reasons: (1) limited space available between two legs of the patient (when on the operating table in lithotomy position) to insert needle through the perineum, and (2) needle is to be penetrated through several layers of different types of tissues (skin, perineum muscles, bulbospongiosus tissue, fascia tissue, prostate capsule, prostate tissue, etc. [5] which exert variable forces.

The size of the perineal wall through which the needles are inserted during PSI is about 6cm x 6cm square and the maximum area of the robot workspace projected on the perineal wall ranges from about 8cm x 8cm to 10cm x 10cm (considering the drape on the patient's body). Therefore, the workspace for the robotic system with needle insertion mechanism is quite limited. To develop a robotic system that can work effectively in this constrained space requires optimum design of components and judicial selection of motors and accessories. Therefore, it is important to know the maximum force that the needle may encounter to reach any targeted position in the prostate to deliver radioactive seeds. Moreover, the needle traverses through different types of tissues and organs to reach the target and these tissues and organs have different types of boundary conditions that cannot be assessed from experimental data obtained from *ex vivo* tissue/organ samples. Therefore, *in vivo* measurement of needle insertion force is useful in designing and controlling any robotic system that will work in such a severely constrained space.

Several researchers have reported needle insertion forces and developed soft tissue models while the insertions have been performed mainly in soft material phantoms like polyvinylchloride (PVC) [6], gelatin [7], silicon rubber [8], and *ex vivo* animal tissues such as bovine liver [9], [10]porcine liver [11], [12], chicken breast [13] and canine prostate [14].

However, perhaps none of the existing models, either empirical or analytical including finite element model (FEM), along with *ex vivo* measurements can accurately assess the forces and tissue deformations while the needle is inserted into the prostate gland through different types of organs and tissues. But, to the best of our knowledge, to date, no *in vivo* force measurement data for needle insertion in human soft tissue, especially in prostate gland, has been reported. Therefore, in this study we have measured and quantified *in vivo* needle insertion forces and motion profiles during prostate brachytherapy in the operating room (OR), which will help us in designing and controlling our Robot-Assisted Platform for Intratumoral Delivery (RAPID) that is being developed.

II. EXPERIMENTAL SETUP

Experimental setup:

We have designed and fabricated a 6 DOF robotic system for needle insertion experiment (see Figure 2).

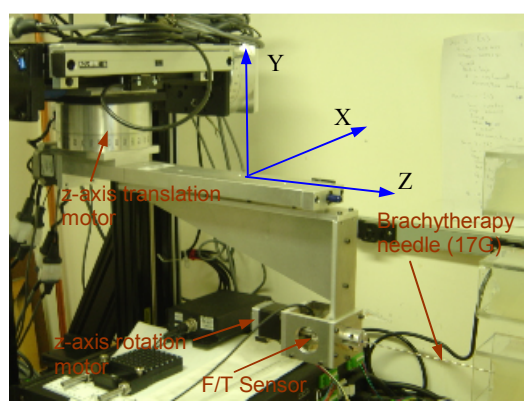

Figure 2: 6 DOF robotic test-bed equipped with a 6 DOF force/torque sensor (Nano25^{TM}).

All the motions (3 positions and 3 orientations) are actuated by stepper motors. Two linear optical

encoders that allow 1μm resolution are mounted on x-axis, and y-axis. A rotary optical encoder with 5μm resolution is fitted on z-axis. The rotational positions about x-axis and y-axis are also monitored by optical encoders that allow 5μm resolutions. The sixth stepper motor actuates the rotation about z-axis, which is intended for studying the effects of rotational oscillations as well as full rotation of the needle. The z-axis, i.e. the direction of needle insertion is made horizontal because in actual prostate brachytherapy in the operating room (OR), the needles are inserted horizontally.

A 6 DOF force-torque (F/T) sensor, (Nano25™ SI-125-3 ® from ATI), is mounted horizontally aligning its z-axis parallel to the robot's z-axis. Maximum force and torque measurement capacities of the F/T sensor are: F_x=125N, F_y=125N, F_z=500N, T_x=3N.m, T_y=3N.m, and T_z=3N.m. The system is kinematically controlled; commands are sent using LabVIEW™ (version 7.1 from National Instruments). The software is executed on Windows XP in a Pentium® 4, 1.6GHz computer with graphical user interface (GUI), which we developed.

Material and method:

We have acquired force/torque (F/T) and position data from real patients in the OR using a hand-held adapter (Figure 3), that we designed and developed, equipped with a 6 DOF F/T sensor. In this *in vivo* measurement, the needle progression into the soft tissue (perineum, prostate and other organs) is registered using ultrasound (US) imaging technique. A 6 DOF electromagnetic (EM)-based position sensor (miniBIRD® from Ascension Technology Corporation) is attached to the hand-held adapter to measure 3D positions and orientations of the F/T sensor and the corresponding time stamps are recorded automatically for calculating the needle insertion velocity and acceleration. To have synchronized data, we have integrated EM-based position sensor (miniBIRD®) with the F/T sensor (Nano25™) so that F/T sensor can trigger the position sensor. We have collected F/T data during prostate brachytherapy procedure in compliance with the Research Subject Review Board (RSRB) approved protocol and with patient's informed consent. In addition to *in vivo* data collected from the OR, we have also gathered *in vitro* data during robotic needle insertion into animal soft tissue phantoms (beef steak wrapped with chicken skin). We have used commercially available brachytherapy needles (similar to those used in the OR) having 1.47mm in diameter (17G) and 200mm in length with diamond tip.

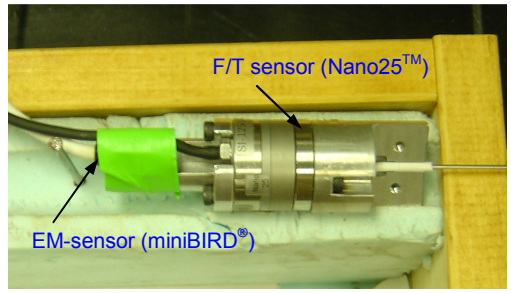

Figure 3: Hand-held adapter equipped with Nano25™ and miniBIRD®.

III. RESULT AND DISCUSSION

Here we present both *in vivo* and *in vitro* data. The time, position, and force data during needle insertion are recorded at a frequency of 100Hz. The F/T data is smoothed using a running average of 20 point-window. The needle velocity and acceleration during manual insertion in the OR as well as in the laboratory are calculated from EM-sensor data. In all the robotic insertion experiments, we used trapezoidal velocity profile for the needle. Both the acceleration and deceleration for the needle motion were 508 mm/s^2. The main portion of the needle motion, the cruising velocity, was 100mm/s.

***In vivo* data:**

We have collected F/T data from different patients in the OR during prostate brachytherapy operation (Figure 4).

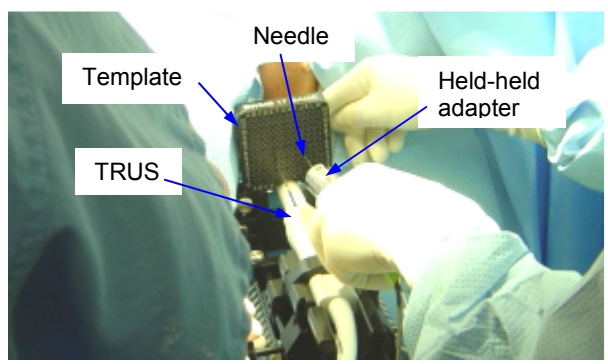

Figure 4: Force/torque and position data collection during actual brachytherapy procedure in the OR.

The hand-held F/T adapter was operated by an experienced surgeon having more than 30 years of surgical experience and 8 years of brachytherapy

experience. An experienced radiologist captured the TRUS images with needle progression through various tissues and organs. We have collected data from 5 patients for 13 needle insertions. Here, we present the needle insertion forces, torques, velocity and surgeon's hand position in Figure 5 through Figure 7 and Table 1. We have also collected needle position data using a 6 DOF EM-based sensor having accuracy of about 1mm. Needle velocity was computed from this 3D position information. The position and velocity and acceleration data are plotted in Figure 8 through Figure 10.

The main force (F_z) profile on the needle during insertion is shown in Figure 5. Since after insertion the needle needs to be in the patient for delivering seeds, we have not presented force data during hand-held adapter retraction. From the graph it is observed that at the initial stage the force increases rapidly and reaches up to about -14N. This peak force is the skin (or perineum wall) puncture force, which is higher than force required to pass through other tissues. After this peak, the force gradually decreases and shows some variations as the needle travels through different tissues and organs. Finally, the needle traverses through the prostate. Total penetration of the needle in the patient is about 8.8cm (from perineal wall up to base of the prostate).

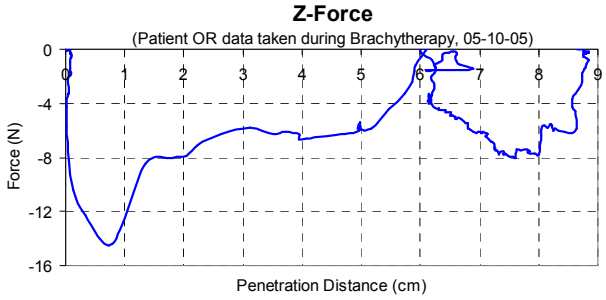

Figure 5: Force (F_z) on the needle when inserted in the patient during brachytherapy procedure in the OR.

The resultant (F_{rt}) of two transverse forces (F_x and F_y) is plotted in Figure 6. From this plot we can notice significant transverse force (about 1.6N) on the needle. We also observe some torques about x-axis and y-axis, but hardly any torque about z-axis (Figure 7). These may be due to the combination of lateral forces exerted by the template, heterogeneous tissues, and needle pre-bending. All of these may arise from different factors including inconsistency of human operation of the needle. It is of interest to note that this force is proportional to (or consistent with) velocity of the needle (Figure 8) and the surgeon's hand movements (Figures 9 & 10).

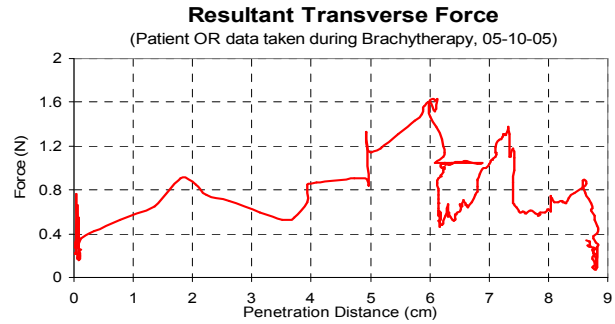

Figure 6: Resultant transverse force (F_{rt}) on the needle when manually inserted in the patient during brachytherapy procedure in the OR.

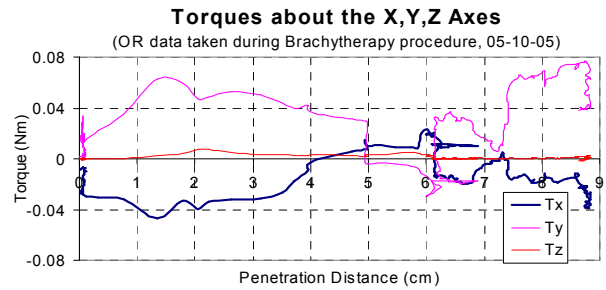

Figure 7: Torques ($T_{x,y,z}$) about x, y, & z axes of the needle when inserted in the patient during brachytherapy procedure in the OR.

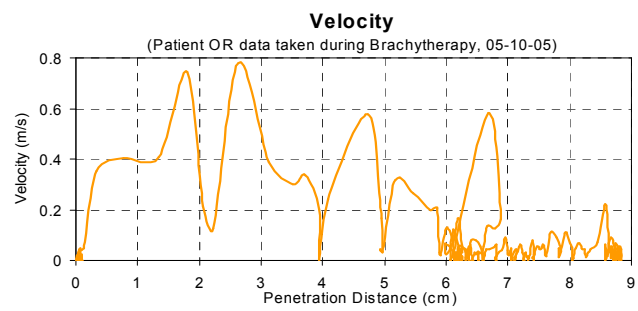

Figure 8: Velocity of the needle when inserted in the patient during brachytherapy procedure in the OR.

From Figure 8, we observe that the maximum needle insertion velocity is about 0.98m/s. At the initial stage of the penetration, the needle velocity is quite high. During this time, the average velocity is about 0.3m/s. In the later stage of the penetration (when the needle is in prostate), the velocity decreases significantly with some peaks. It appears that the needle holder's movement in x-y plane can be reduced significantly by deploying a robotic system to insert needle under a surgeon's supervision. In turn, this will reduce the needle bending and will enhance targeting accuracy. Data collected from 5 patients

have been summarized in Table 1. We observe the average insertion forces about 15N and 7N in perineum and prostate, respectively; and the average insertion velocity is about 0.9m/s. It may be difficult to achieve this type of high velocities while using a robot to insert needle during PSI procedures. However, significantly lower insertion velocity (about 10cm/s) may be sufficient and safe for robotic insertions.

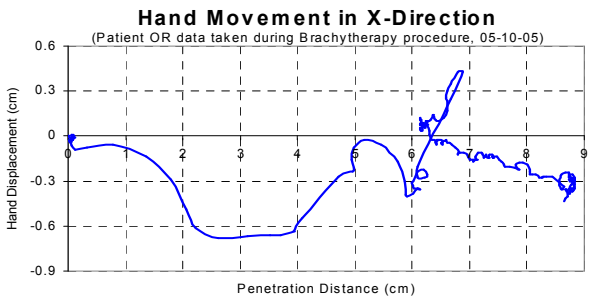

Figure 9: Surgeon's hand movement in x-direction.

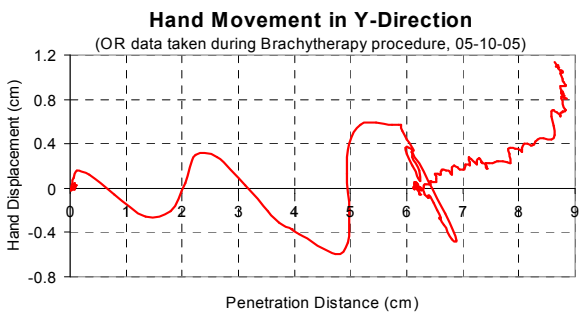

Figure 10: Surgeon's hand movement in y-direction.

Table 1: Summary of *in vivo* data collected from OR.

Patient	Max. Force in Perineum (N) (Avg./SD)	Max. Force in Prostate (N) (Avg./SD)	Max. Velocity (m/s) (Avg./SD)
Patient #1	15.63/ 2.74	8.24/ 2.72	0.65/ 0.42
Patient #2	16.85/ 4.45	5.95/ 0.64	1.17/ 0.40
Patient #3	13.87/ 3.53	7.93/ 2.57	0.94/ 0.16
Patient #4	15.26/ 4.61	5.72/ 0.95	0.98/ 0.01
Patient #5	14.22/ 4.03	6.85/ 1.09	0.86/ 0.08
Patient #1-5	**15.03/ 3.26**	**7.11/ 1.92**	**0.89/ 0.28**

***In vitro* data:**

We have performed several experiments with robotic and manual needle insertions into soft animal tissues (beef steak wrapped in chicken skin). The main insertion force (F_z) and the resultant transverse force (F_{rt}) are presented in Figures 11 and 12, respectively. The maximum penetration is about 14cm and the velocity is 10cm/s. All these data are the average of five insertions at different locations of the meat sample. From Figure 11, it is noticed that F_z forces in human insertion and in robotic insertion are comparable. We notice a sharp rise in F_z force for beef wrapped in chicken skin (first part in Figure 11). This sudden change in force profile is attributed to the chicken skin puncturing. The beef roast was wrapped with chicken skin in an attempt to mimic the human perineum/skin. But it appears that the F_z force increases and drops more sharply as compared to human skin/perineum. This may be due to the lack of good attachment of chicken skin to beef roast. After this initial phase, the force increases gradually as a contrast to *in vivo* measured force (Figure 5). This difference is attributed to mainly two factors (1) in OR, the needle was inserted with very high acceleration (about 30m/s^2), which contributed to large inertia force, and (2) after insertion into perineum, the surgeon paused (or slowed down) quite often to check the ultrasound images to track needle position (Figure 8), during these pauses the tissues/organs relaxed significantly resulting in reduction in insertion force.

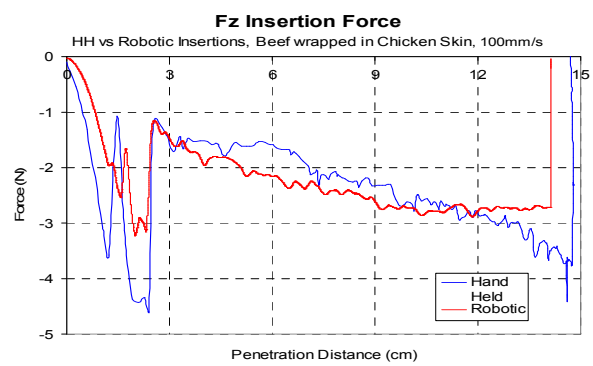

Figure 11: Main insertion force (F_z) – robotic (red color), manual (blue color).

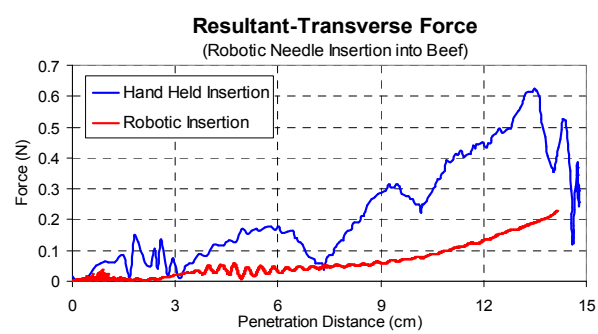

Figure 12: Resultant transverse force (resultant of F_x and F_y) – robotic (red color), manual (blue color).

In Figure 12, as one would expect, we noticed that resultant transverse force (F_{rt}) in robotic needle insertion is more and fluctuating as compared to manual insertion. The F_{rt} in robotic insertion is gradually increasing because of some misalignment

between the template hole and the needle holder. We can observe similar pattern for torques about x-axis and y-axis (Figure 13); hardly any torque was experienced about z-axis.

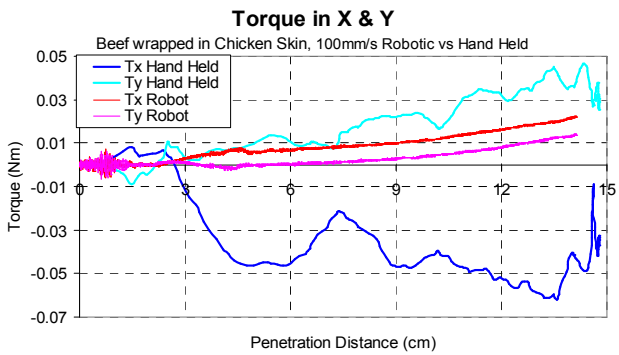

Figure 13: Torques about x-axis and y-axis (T_x and T_y) – robotic (red & magenta), manual (blue & cyan).

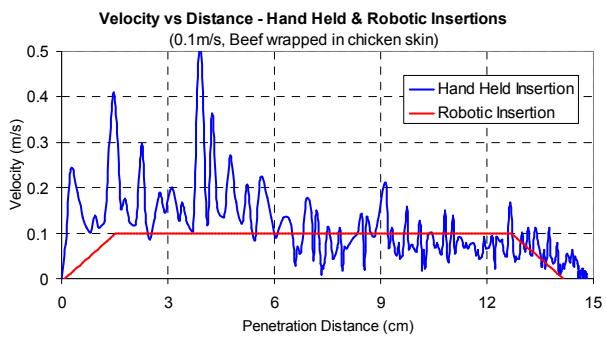

Figure 14: Needle insertion velocities – robotic (red color), and manual (blue color).

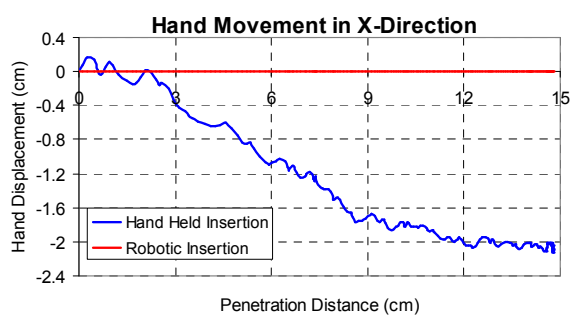

Figure 15: Needle holder's movement in x-direction – robotic (red color), and manual (blue color).

Needle insertion velocities for robotic insertion and for manual insertion are compared in Figure 14. Robot was instructed to move at a cruising speed of 10cm/s, and the human operator tried to produce the same speed. But, as we can see, the manual insertion speed fluctuated roughly between 5cm/s and 30cm/s (Figure 14). From Figure 15 and Figure 16 we observe needle holder's positions in x-y plane for robotic insertion are much more consistent as compared to that of manual insertion. As a result of unsteady motion, the targeting accuracy of manual insertion is inferior to robotic insertion (Figures 17 & 18). The average positional errors of the needle tip are 1.5mm and 0.6 9mm for manual and robotic insertion, respectively (Table 2).

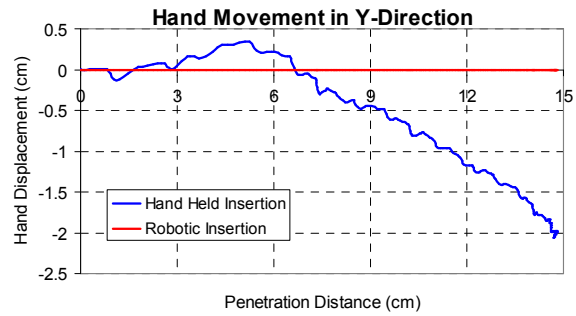

Figure 16: Needle holder's movement in y-direction – robotic (red color), and manual (blue color).

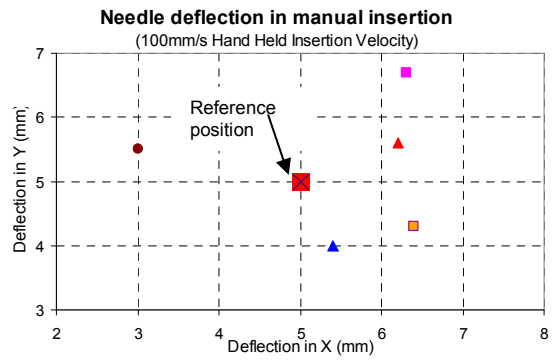

Figure 17: Position error of the needle tip for manual insertion (poor repeatability and accuracy).

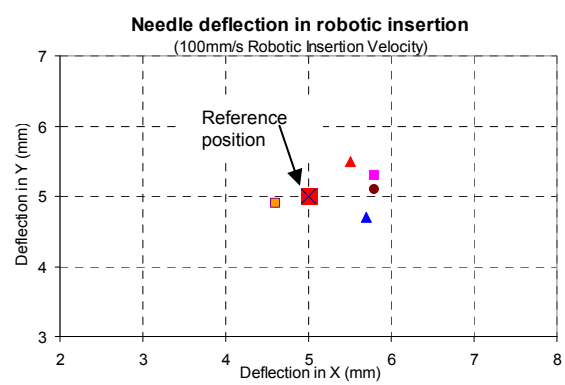

Figure 18: Position error of the needle tip for robotic insertion (good repeatability and accuracy).

Table 2: Targeting errors in manual insertions and in robotic insertions.

Insertion	Avg. x-error (mm)	Avg. y-error (mm)	Avg. target error (mm)
Manual	1.26	0.90	1.55
Robotic	0.64	0.26	0.69

IV. CONCLUSION AND FUTURE WORK

In this paper, we have presented both *in vivo* and *in vitro* force, torque, velocity and position profile data. *In vivo* data is collected from 5 patients during prostate brachytherapy procedure in the OR. The force-torque data has been collected using a 6 DOF force-torque sensor. The needle position has been recorded using a 6 DOF EM-based sensor. The *in vivo* data reveals that average maximum needle insertion force is about 15N, and the average maximum velocity is about 0.9m/s. We observe significant transverse force on the needle (avg. max. about 1.2N). From *in vitro* data it is observed that robotic needle insertion is more accurate and consistent as compared to manual insertion, which in turn will enhance the treatment quality.

These *in vivo* data present some useful insights into the force and torque on the needle, and needle velocity on during actual brachytherapy procedure in the OR. We will be considering the *in vivo* as well as *in vitro* force-torque, and motion profile data and knowledge in designing and controlling a robotic system for prostate brachytherapy. We are in the process of collecting more *in vivo* data from different patients and studying the effects of patient specific criteria such as age, height, body mass index (BMI), prostate specific agent (PSA) value, special anatomy, etc. on needle insertion force-torque to evolve optimized control parameters for the robotic system.

ACKNOWLEDGEMENT

This work is supported by the National Cancer Institute (NCI), under grant R01 CA091763. The authors would like to thank Mr. Dave Fuller in collecting data presented in this paper.

REFERENCE

[1] American Cancer Society (ACS), "*Cancer Facts & Figures 2005*, http://www.cancer.org/docroot/STT/stt0.asp, website accessed in June 2005.

[2] G. Fichtinger, T. L. DeWeese, A. Patriciu, A. Tanacs, D. Mazilu, J. H. Anderson, K. Masamune, R. Taylor, and D. Stoianovici, "System for Robotically Assisted Prostate Biopsy and Therapy with Intraoperative CT Guidance, in the Journal Academic Radiology, Vol. 9, pp. 60-74, 2002.

[3] Z. Wei, G. Wan, L. Gardi, D. B. Bowney, and A. Fenster, "Robotic Aided 3D TRUS Guided Intraoperative Prostate Brachytherapy, in the *Proceedings of SPIE*, Vol. 5367, pp. 361-370, Bellingham, WA, 2004.

[4] D.M. Elliot, J. J. Berkey, G. M. Hoedeman, "Automated Implantation System for Radioisotope Seeds, *United States Patent No. US 006869390B2*, March 2005.

[5] P. L. Williams, and R. Warwick, "*Gray's Anatomy*, 36th Edition, edited by W. B. Saunders Company, New York, 1980.

[6] S. P. DiMaio, and S. E. Salcudean, "Needle Insertion Modeling and Simulation, in *the IEEE Trans. on Robotics and Automation*, Vol. 19, No. 5, pp. 864-875, Oct. 2003.

[7] L. Hiemenz, A. Litsky, P. Schmalbrock, "Puncture Mechanics for the Insertion of an Epidural Needle, presented at the *21st Annual Meeting of the American Society of Biomechanics*, Clemson University, SC, 1997.

[8] A. M. Okamura, C. Simone, and M. D. O'Leary, "Force Modeling for Needle Insertion into Soft Tissue, in *the IEEE Transactions on Biomedical Engineering*, Vol. 51, No. 10, Oct. 2004.

[9] M. D. O'Leary, C. Simone, T. Washio, K Yoshinaka, and A. M Okamura, "Robotic Needle Insertion: Effect of Friction and Needle Geometry, in *the Proceedings of the IEEE Int. Conference on Robotics and Automation*, pp. 1774-1779, Taipei, Taiwan, Sept. 2003.

[10] C. Simone and A.M. Okamura, "Modeling of Needle Insertion Forces for Robot-Assisted Percutaneous Therapy, in *the Proc. of the IEEE Int. Conference on Robotics and Automation*, pp. 2085-2091, Washington, DC, May 2002.

[11] P. Brett, A. J. Harrison, and T. A. Thomas, "Scheme for the Identification of Tissue Types and Boundaries at the Tool Point for Surgical Needles, in *the IEEE Transactions on Information Technology in Biomedicine*, Vol. 4, No. 1, pp. 30-36, March 2000.

[12] M. P. Ottensmeyer, and J. K. Salisbury, "In Vivo Data Acquisition Instrument for Solid Organ Mechanical Property Measurement, in *the MICCAI (LNCS* Vol. 2208, pp. 975 -982), Utrecht, Netherlands, Oct. 2001.

[13] K. Yan, W. S. Ng, K. V. Ling, T. I. Liu, Y. Yu, and W. Odell, "Literature Review on Needle Guidance in Soft Tissue and Preliminary Work on Smart Needling, in the *Proceedings of IEEE Conference on Robotics, Automation and Mechatronics*, pp. 49-54, Singapore, 2004.

[14] H. Kataoka, T. Washio, K. Chinzei, K. Mizuhara, C. Simone, and A. M. Okamura, "Measurement of the Tip and Friction Force Acting on a Needle during Penetration, in *the MICCAI (LNCS*, Vol. 2488, pp. 271-278), Tokyo, Japan, Sept. 2002.